

---

## **Advances in laser forming of metal foam: mechanism, prediction and comparison**

---

Tizian Bucher\* and Y. Lawrence Yao

Department of Mechanical Engineering,  
Advanced Manufacturing Laboratory,  
Columbia University,  
New York, NY 10027, USA  
Email: tb2430@columbia.edu  
Email: yly1@columbia.edu  
\*Corresponding author

**Abstract:** Laser forming is a well-studied process that has successfully been used to form sheet metal. More recently, attempts have been made to use laser forming to bend metal foams. While several studies reported that forming of metal foams is possible, it was found that the process window is fundamentally different, and many well-established concepts from sheet metal laser forming do not apply or require modification. This paper reviews the advances in metal foam laser forming and compares the acquired knowledge with the well-established knowledge of sheet metal laser forming. Differences in the bending mechanism are discussed, and the process windows are analysed in detail. Additionally, key differences in the numerical approaches are discussed, namely the impact of the model geometry and the incorporation of density-dependent material data. Finally, subjects requiring further investigation are reviewed.

**Keywords:** laser forming; metal foam; bending mechanism; process window; numerical simulation.

**Reference** to this paper should be made as follows: Bucher, T. and Yao, Y.L. (2018) 'Advances in laser forming of metal foam: mechanism, prediction and comparison', *Int. J. Mechatronics and Manufacturing Systems*, Vol. 11, Nos. 2/3, pp.250–273.

**Biographical notes:** Tizian Bucher is a PhD candidate in Mechanical Engineering at Columbia University.

Y. Lawrence Yao is a Professor of Mechanical Engineering at Columbia University.

---

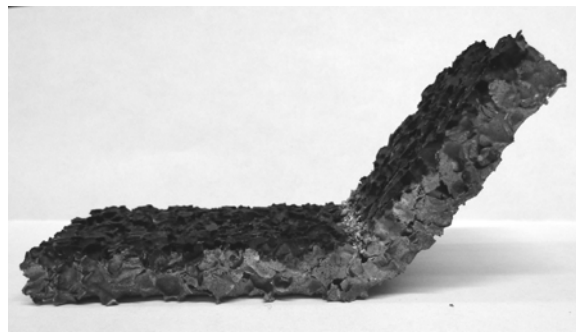
### **1 Introduction**

Laser forming is a method that allows bending materials without establishing contact or requiring moulds. The process is well understood when used on solid sheet metal, and many aspects have been studied in great detail, such as the governing bending mechanisms (Vollertsen, 1993), effects of different strain rates (Li and Yao, 2000) and

cooling schemes (Cheng and Yao, 2001), as well as aspects relating to 3-dimensional forming (Edwardson et al., 2005a) and process synthesis (Cheng and Yao, 2004).

In this decade, laser formed started being used to bend metal foam. Metal foam is a relatively new type of material that has an excellent shock absorption capacity and a high strength-to-weight ratio (Ashby et al., 2000). Due to these unique properties, metal foam excels in many applications such as crash absorbers in cars, as well as structural components in solar power plants and aerospace equipment (Banhart, 2001). Laser forming studies have been performed with different types of metal foams, such as open-cell foams (Quadrini et al., 2010), closed-cell foams (Zhang et al., 2015; Bucher et al., 2016, 2017), and closed-cell foams with protective skins (Guglielmotti et al., 2009), all reporting that laser forming is capable of bending metal foams up to 45° and beyond. An example for closed-cell aluminium foam is shown in Figure 1. Unlike solid sheet metal, which can be bent efficiently and cost-effectively in numerous alternative fashions, metal foam can only be bent successfully using laser forming. Three point bending, for instance, causes many types of failures at low bending angles (D'Urso and Maccarini, 2011), and hydroforming densifies the material (Mata et al., 2013). Near-net-shape processes, such as powder metallurgy processes (Claar et al., 2000) or 3D printing (Kennedy, 2012), are no valid alternatives either, since the former requires moulds and is limited to small parts with large production volumes, whereas the latter is inherently slow and limited to very small part sizes. Hence, laser forming has a great potential, since it allows for the manufacture of metal foam parts with complex curvatures and arbitrary sizes without tool wear (Bucher et al., 2016, 2017).

**Figure 1** Closed-cell aluminium foam after 250 laser scans performed with a power of 180 W, scan speed of 10 mm/s, and laser diameter of 12 mm. Bending angles of 45° and greater are feasible over single scan lines



Within the last few years, a lot of progress has been made towards a better understanding of laser forming of metal foams. While different studies have shown that lasers can successfully bend metal foam, it has nonetheless become apparent that metal foam behaves fundamentally different than sheet metal during laser forming. Experimentally, it has been shown that the process window used for metal foam greatly differs from the process window used for solid sheet metal. Moreover, the bending mechanisms, identified by Vollertsen (1993) for sheet metal laser forming, are either not valid or require modification. Finally, the numerical simulation of the process becomes more complex when moving to metal foam, since aspects related to the foam geometry and densification need to be considered.

In this study, the advances in the field of metal foam laser forming are reviewed, and the acquired knowledge is contrasted with the well-established knowledge of sheet metal laser forming. The analysis is started with a discussion of the bending mechanisms, followed by an analysis of the differences and similarities in the process windows and simulation approaches. Finally, topics requiring further research are reviewed.

## 2 Bending mechanism

Laser forming is a thermo-mechanical process that involves laser-induced heating and subsequent mechanical deformation via thermal expansion. Depending on the process conditions, the thermal and mechanical response of the treated material differs, giving rise to different bending mechanisms. For solid sheet metal, three major bending mechanisms have been identified (Vollertsen, 1993):

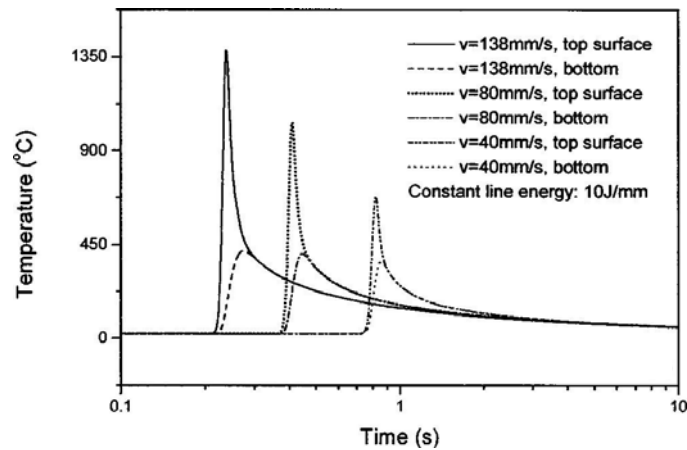
- 1 The temperature gradient mechanism (TGM) governs the scenario where the laser diameter is small compared to the sheet thickness. During the laser scan, a steep temperature gradient develops across the sheet thickness, and only a small material segment right underneath the laser source undergoes significant heating. The heated segment tries to expand, but is restricted by the 'cold' surrounding material. Instead of expanding, the material undergoes plastic compression. This plastic compression occurs along the entire laser scan, shortening the material near the top surface relative to the material near the bottom surface, thereby bending the sheet towards the laser.
- 2 The buckling mechanism (BM) governs when the laser source is large compared to the sheet thickness. In that scenario, the processed material heats up uniformly throughout the thickness. The thermal expansion of the heated area is again restricted by the cold surrounding material, and high compressive stresses develop. Due to the uniform heating and the low sheet thickness, however, the material can relax some of the compressive stresses by buckling either towards or away from the laser. Once buckling initiates, the buckled region is translated along the laser scan line, eventually bending the sheet in the direction opposite to the buckling direction.
- 3 The upsetting mechanism (UM), governs the same scenario as the BM, except that buckling is geometrically restricted, as is for instance the case in tubes (Li and Yao, 2001a). Instead of buckling, the material thickens, whereby thickening is slightly more pronounced near the top surface than the bottom surface. Due to that imbalance, the sheet bends towards the laser.

Several modifications of the aforementioned mechanisms have been proposed over time, such as the coupling mechanism CM (Shi et al., 2006), or the martensite expansion mechanism MEM and the residual stress relaxation mechanism RSRM (Pretorius, 2009), which are not discussed in detail since their validity has not yet been investigated for metal foams.

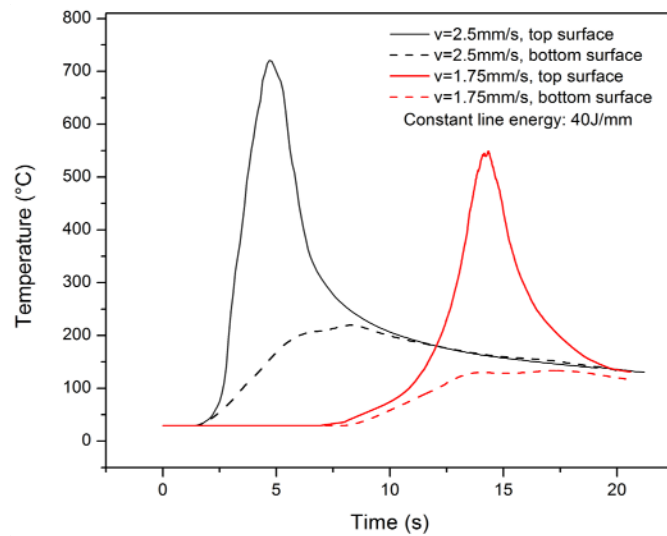
When transitioning from solid metal sheets to metal foam, the previously discussed bending mechanisms are either not valid or require modification. The BM, for instance, cannot occur in metal foams, since buckling requires large compressive stresses that would crush the fragile foam structure (Bucher et al., 2017). Moreover, metal foams generally have a large sheet thickness as well as a high geometry-induced stiffness that

render buckling impossible. The UM is also highly unlikely to occur, since it requires uniform heating throughout the thickness and thickening. The former is difficult to achieve due to the large sheet thickness, and the latter is restricted by the high moment of area of the foam (Guglielmotti et al., 2009).

**Figure 2** Temperature history plots at constant line energies for (a) a steel sheet (numerical results) that is laser formed using TGM conditions (Li and Yao, 2000) and (b) an aluminium foam (experimental results), laser formed at typical process conditions (see online version for colours)



(a)



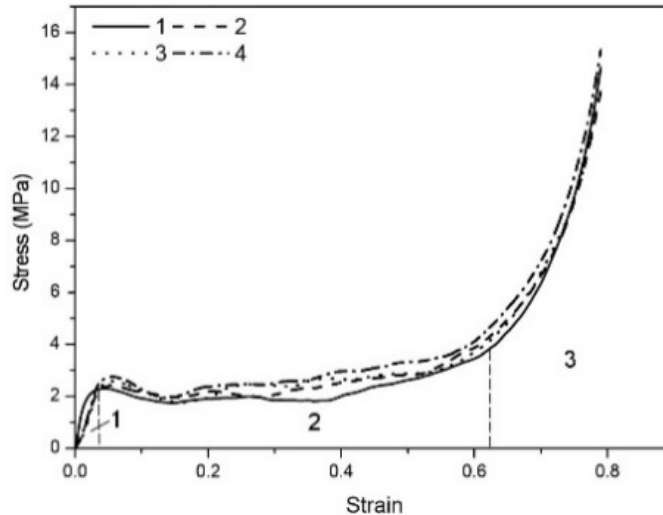
(b)

Notes: In both cases, there are large temperature differences between the top to the bottom surfaces, indicating the presence of a steep gradient. The temperature history profiles of metal foam closely resemble the temperature history profiles of steel during typical TGM conditions.

The TGM has long been assumed to be the governing bending mechanism, owing to the fact that temperature gradients can easily be induced in metal foams. Experimental investigations confirmed that steep temperature gradients develop in foams [Figure 2(b)], which are similar to the temperature gradients occurring in steel sheets during typical TGM conditions [Figure 2(a)]. Additionally, it was shown that metal foams yield small Fourier numbers ( $Fo = D\alpha / vt^2$ ) compared to solids, due to their large sheet thicknesses (Bucher et al., 2016). Hence, from a thermal perspective, metal foam satisfies the prerequisites for the TGM.

From a mechanical standpoint, on the other hand, metal foam does not satisfy the criteria of the TGM, for several reasons. Firstly, the TGM requires high compressive stresses that give rise to plastic compressive strains. Such compressive stresses cannot develop in metal foam, because it collapses and densifies as can be seen from the compressive stress-strain curve (Figure 3). High compressive stresses can only develop once the metal foam is fully densified, represented by stage 3 in Figure 3. Experiments confirmed that cell walls bend outwards during laser forming, especially within the top half of the specimen (shown by arrows in Figure 4), clearly indicating that the cell walls are unable to withstand the compressive stresses that develop.

**Figure 3** Typical uniaxial compression stress-strain curves of a closed-cell metal foam



Notes: The stress-strain curve can be divided into three segments: (1) a linear regime, followed by (2) a plateau where cell crushing occurs and a large amount of energy is absorbed, followed by (3) foam densification. Due to their crushability, metal foams can yield hydrostatically and withstand much lower compressive stresses than solid metals.

Source: Haijun (2007)

**Figure 4** Cross-section of a foam specimen after 5 laser scans at a power of 180 W and a scan speed of 10 mm/s (see online version for colours)



Notes: The laser was scanned into the page. Several cell walls were bent during the laser scans (shown by white arrows), indicating that the foam cannot withstand high compressive stresses.

Source: Bucher et al. (2017)

Secondly, thin cell walls undergo some melting, regardless of how low the laser power is chosen (Bucher et al., 2017). Melting initiates at the first scan and continues until either the entire cell wall is melted, or the cell wall thickness increases. If the TGM were truly based on plastic compressive strains, melting would drastically decrease the amount of bending, because it reduces the amount of compressible material. Experiments have shown, however, that melting hardly impedes the bending deformation, giving an additional argument against the validity of the traditional TGM.

**Figure 5** The moment of area (about  $z = 0$ ) of a metal foam with 89% porosity is 43.4 times higher than the area moment of a solid with the same cross-sectional area

	Cross-section	Moment of area
Solid		1
Foam		43.4

Note: Hence, foams have a high geometry-induced stiffness to bending deformation.

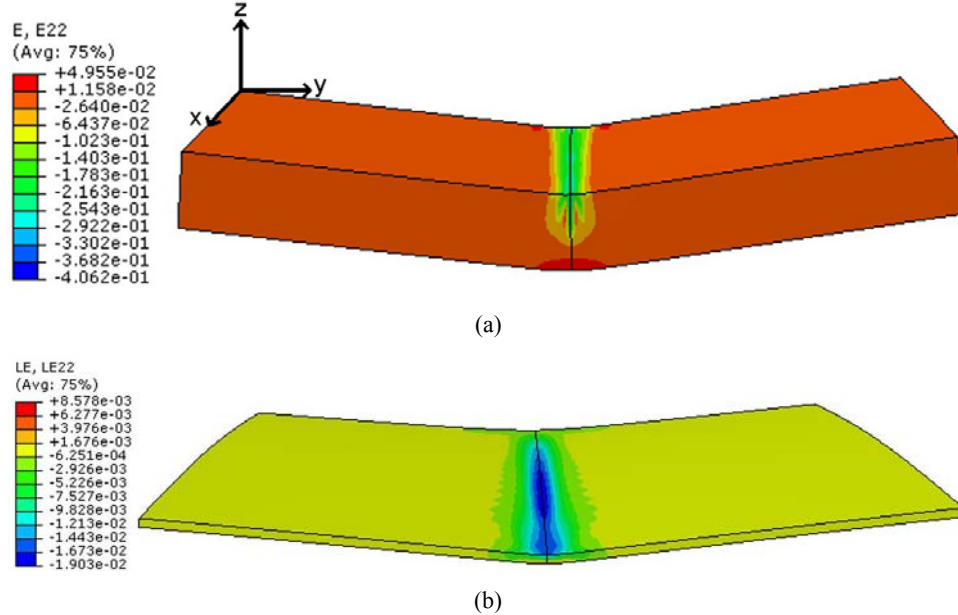
Source: Bucher et al. (2017)

Finally, the TGM does not explain why metal foam can bend despite its high bending stiffness and poor tensile formability. The TGM predicts that compression-induced shortening occurs near the top surface. To accommodate this shortening, the remaining section needs to bend mechanically, and tensile stresses need to develop near the bottom surface. Mechanical bending of metal foam is prohibitively difficult since its moment of area is more than an order of magnitude greater than the moment of area of a solid with the same cross-sectional area as shown in Figure 5. Moreover, it has been shown that metal foams fail prematurely when loaded in tension (Haijun, 2007; Zu et al., 2013).

Considering all these arguments against the validity of the TGM, it is tempting to think that bending occurs via a mechanism that is not dominated by plastic compressive deformation, but that is instead dominated by heat-induced softening and subsequent tensile stretching. Numerical results have shown, however, that compressive deformation is prevalent in both solids and foams during laser forming. As shown in Figures 6(a) and 6(b), compressive plastic strains ( $\epsilon_{yy}$ ) occur throughout the top 80% of the solid and foam cross-sections, respectively, and tensile deformation is limited to a small segment on the bottom surface. Moreover, the ratio of compressive strain (on top surface) to tensile strain (on bottom surface) are almost equal in both cases (Bucher et al., 2017).

Therefore, the bending deformation during laser forming is always dominated by compressive deformation, leaving only one possible conclusion: the cell collapse observed in metal foams (see Figure 4) is equivalent to the plastic compressive strains observed in sheet metal.

**Figure 6** Strain distributions ( $\epsilon_{yy}$ ) in (a) metal foam and (b) a steel sheet after a laser scan (see online version for colours)



Notes: The steel sheet was laser formed at typical TGM processing conditions. In both cases, the deformation near the laser scan line is compressive over the majority of the thickness. Hence, compressive deformation is the main cause of bending.

Source: Bucher et al. (2017)

Based on this key difference, a new bending mechanism was proposed that was called ‘modified temperature gradient mechanism’ (MTGM). Just like the TGM, the MTGM postulates that steep temperature gradients develop across the sheet thickness, which give rise to compressive shortening near the top surface. Instead of shortening due to plastic compressive strains, however, the MTGM postulates shortening through cell wall bending and cell collapse. The cell collapse, in turn, causes the foam to densify, which is another new aspect of the MTGM. In the MTGM, some tensile deformation also occurs on the bottom surface, but the tensile strains are small, and immediate fracture is prevented by heat-induced softening.

The bending behaviour at a high number of laser scans is very similar for specimens bent through the TGM and the MTGM, as shown in Figures 7(a) and 7(b), respectively. In both cases, the bending increment decreases with an increasing number of scans, and there is a maximum achievable bending angle for each process condition. However, the reason for the plateau behaviour is different for solids and metal foams. In solids, the bending limit is caused by thickening, strain hardening, and changes in the laser absorption (Edwardson et al., 2006). In metal foams, on the other hand, thickening does not occur. Tensile strain hardening is negligible since the tensile strains are comparatively small in magnitude, and compressive hardening does not occur due to the plateau shape of the compression curve (Figure 3). Changes in the laser absorption do occur, but have a negligible impact. Instead, the limit is mostly caused by densification, i.e., an increase in the relative density ratio  $\rho_f / \rho_s$ , which in turn increases the Young’s modulus,  $E$  (Mondal et al., 2007), the flow stress,  $\sigma$  (Gibson and Ashby, 1988), and the thermal conductivity,  $k$  (Ashby et al., 2000):

$$\frac{E_f}{E_s} = \frac{(1 - \rho_f / \rho_s)^2}{(1 + (2 - 3\nu_s) \rho_f / \rho_s)} \quad (1)$$

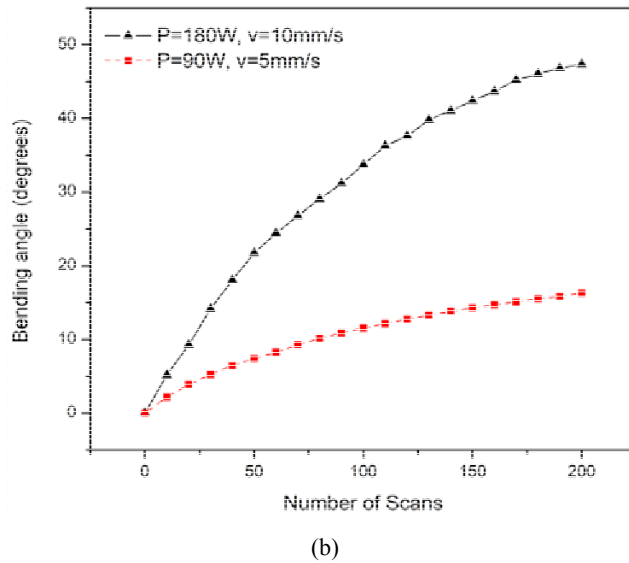
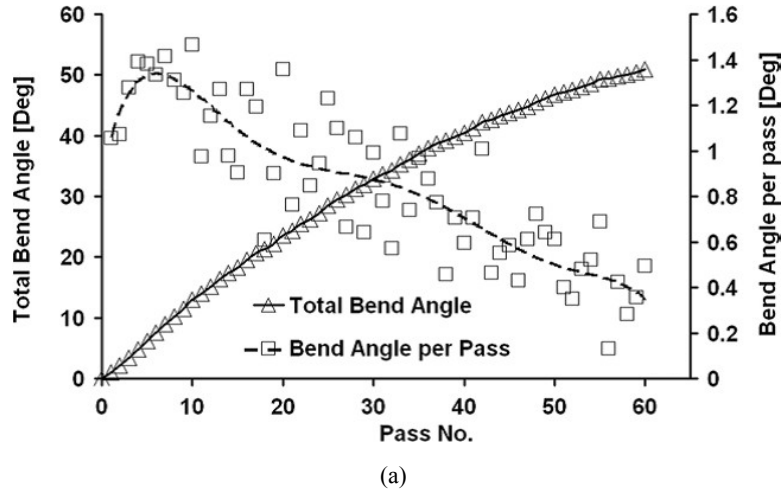
$$\frac{\sigma_f}{\sigma_s} \approx 0.3 \left( \phi \frac{\rho_f}{\rho_s} \right)^{3/2} + (1 - \phi) \frac{\rho_f}{\rho_s} \quad (2)$$

$$\left( \frac{\rho_f}{\rho_s} \right)^{1.8} < \frac{k_f}{k_s} < \left( \frac{\rho_f}{\rho_s} \right)^{1.65} \quad (3)$$

where  $\nu$  is Poisson’s ratio,  $\phi$  is the percentage of solid material at cell intersections, and the subscripts ‘ $f$ ’ and ‘ $s$ ’ refer to the foam and solid properties, respectively. An increase in the thermal conductivity increases the heat conducted through the foam, thereby reducing the temperature gradients and decreasing the driving force for cell collapse. Similarly, an increase in the moment of area renders the foam stiffer to bending deformation, and an increase in the flow stress reduces the plastic strain formation for a given stress state.

From Figures 7(a) and 7(b), it is further apparent that it takes much more laser scans to bend a 10 mm thick metal foam sheet by the same angle as a 1.5 mm thick solid steel sheet. The reduced efficiency of the MTGM compared to the TGM is both due to the foam’s larger sheet thickness, as well as its higher geometry-induced stiffness (see Figure 5).

**Figure 7** Bending curves for (a) a 1.5 mm thick steel sheet (Edwardson et al., 2006), laser formed using TGM conditions and (b) a 10 mm thick aluminium foam sheet, laser formed at two conditions with constant line energies (see online version for colours)



Note: In both cases, the bending increment decreased with an increasing number of scans, but the reason for the limiting behaviour differed.

### 3 Process conditions

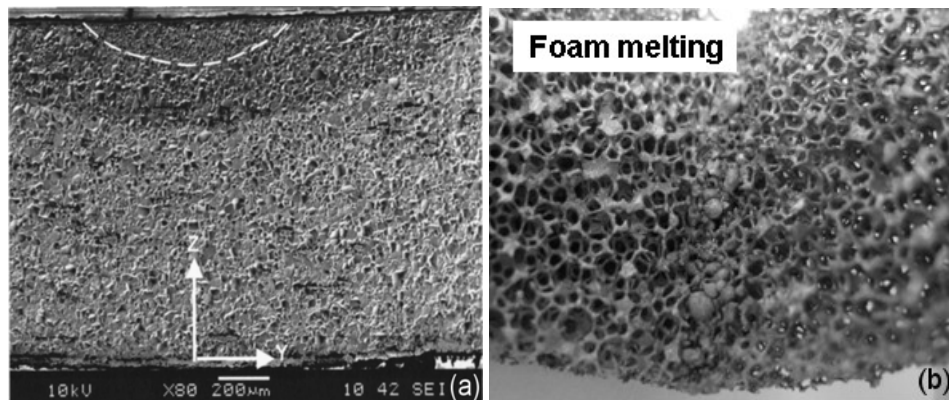
Solid and foamed metals require fundamentally different process windows, summarised in Table 1. The process window that is applicable to metal foams is a small subset of the sheet metal process window (with the exception of the scan speed), which is not surprising considering that metal foams can only be bent through a single bending mechanism.

**Table 1** Typical processing conditions used for sheet metal (Li and Yao, 2001b, 2001c; Vollertsen, 1993; Scully, 1987; Masubuchi and Jones, 2000; Edwardson et al., 2005b) and metal foam (Bucher et al., 2016, 2017; Zhang et al., 2015; Roohi et al., 2015; Guglielmotti et al., 2009; Quadrini et al., 2010, 2013; Santo et al., 2010, 2012)

Property	Units	Solid	Foam
Power, $P$	W	50–13,000	50–350
Scan speed, $v$	mm/s	10–600	1.8–15
Spot size, $D$	mm	2–25	2–15
Sheet thickness, $s_0$	mm	0.2–25.4	2–25

In general, much higher power levels can be used on sheet metals, for various reasons. First, heat can conduct away from the top surface more easily due to the higher thermal conductivity, and overheating occurs less readily. High temperatures may cause localised grain refinement and hardening [Figure 8(a)], but are for the most part not detrimental to the structural integrity and the mechanical properties. Also, excessive temperatures can be avoided by increasing the sheet thickness and the spot size. Overall, sheet metal can be laser formed with a wide range of process parameter combinations, and over-heating occurs less readily.

**Figure 8** Solid and foamed metals respond differently to elevated temperatures

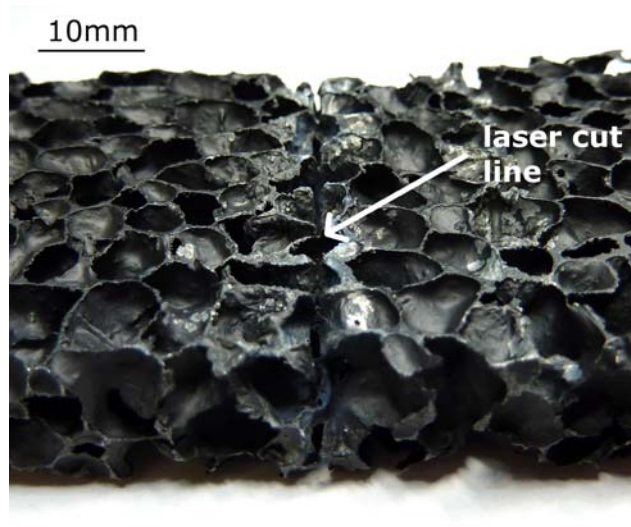


Notes: Sheet metal has a much higher tolerance and can experience grain refinement (area within dashed line) and hardening (darkened area), shown in (a) (Cheng and Yao, 2002). Metal foams, on the other hand, readily melt (visible as droplets) and tarnish as shown in (b), especially near the end of the laser scan line due to laser pre-heating (Santo et al., 2012).

Metal foams, on the other hand, have a much lower thermal conductivity in combination with a fragile cellular structure. As a consequence, heat tends to accumulate near the top surface, causing large temperature rises at the scan line. Therefore, over-heating and melting of thin cellular structures occurs much more readily, shown in Figure 8(b). Avoiding over-heating by increasing the sheet thickness and the spot size is more difficult, since both parameters need to be adjusted perfectly to enable laser forming. Depending on the cavity size, low-density metal foam panels (porosity > 80%) are often not structurally sound below a thickness of around  $s_0 = 10$  mm (high-density foams may also be cut to thinner sheets with a thickness of around  $s_0 = 2$  mm). At the same time, the

sheet thicknesses may not exceed around  $s_0 = 25$  mm, because the geometry-induced stiffness becomes too large. Moreover, higher power levels would be required for laser forming, inevitably causing an excessive amount of melting. Similarly, spot sizes are typically  $D = 6$  mm or greater (with the exception of high-density foams that can use  $D = 2$  mm), or else the foam is cut as opposed to bent (Figure 9). Laser spot sizes are typically also chosen smaller than around  $D = 15$  mm to maintain a sufficient energy intensity while also keeping the heat-affected zone small.

**Figure 9** Metal foam that was scanned with a spot size of 4 mm at a power of 100 W and a scan speed of 5 mm/s



Note: Due to the high energy intensity, the foam was cut at the centre of the laser spot.

Since metal foams require a reduced power, they also need to be laser formed at a lower scan speed to maintain a similar line energy  $LE = P/v$ , reducing the overall productivity of the process. The concept of the line energy, which is supposed to keep the energy influx constant and cause a constant bending angle, does not entirely hold for foams and sheet metal. In sheet metal, it is well accepted that as the input power and the scan speed increase, heat gets ‘trapped’ near the top surface and has less time to dissipate. As a consequence, a higher maximum temperature is reached on the top surface [see Figure 2(a)], causing a higher amount of plastic compressive deformation and thus a larger bending angle (Li and Yao, 2001b). In metal foams, the heat diffusivity is smaller than in solid metal, and the heat always has a tendency to accumulate near the top surface. Nevertheless, an increase in the power and the scan speed still gives rise to the same phenomenon observed in sheet metal, and the top surface temperature increases [Figure 2(b)]. Due to the increased heating near the top surface, more cell wall bending occurs, leading to larger bending angles shown in Figure 7(b). Therefore, the knowledge from sheet metal laser forming regarding the line energy concept directly translates to metal foams.

Foamed and solid metals are also similarly sensitive to the sheet thickness. For solid metal, the bending angle is proportional to the inverse of the thickness squared [Figure 10(a)]. The same proportionality comes out of an analytical relation by Vollertsen (1994) for a TGM condition:

$$\alpha_B = 3 \frac{\alpha_{th}}{\rho c_p} \frac{PA}{v s_0} \frac{1}{s_0} \quad (4)$$

where  $\alpha_B$  is the bending angle,  $\alpha_{th}$  thermal expansion coefficient,  $c_p$  the specific heat capacity,  $P$  the power,  $A$  the absorption coefficient,  $v$  the scan speed, and  $s_0$  the sheet thickness. This relation may not hold for metal foam, because the foam sheet thickness is not interchangeable with the solid sheet thickness due to the porosity of the foam. Nevertheless, it can be shown from analytical relations that the moment of area  $I$  and thus the bending stiffness  $S$  increase to the power squared with an increasing amount of material away from the bending axis (see Figure 5), as shown in:

$$I = \int_{-s_0/2}^{s_0/2} z^2 y(z) dz \quad (5)$$

$$S = \frac{B_1 EI}{l^3} \quad (6)$$

where  $B_1$  is a scaling factor that is boundary and loading condition dependent,  $E$  is Young's modulus, and  $l$  the beam length (Ashby et al., 2000). Therefore, an increase in the thickness renders the foam much stiffer to bending deformation. This was confirmed by experiments shown in Figure 10(b), where a doubled sheet thickness caused a significant drop in the bending angle. Hence, both solid and foamed metals are extremely sensitive to the sheet thickness, and the bending efficiency decreases with increasing sheet thickness.

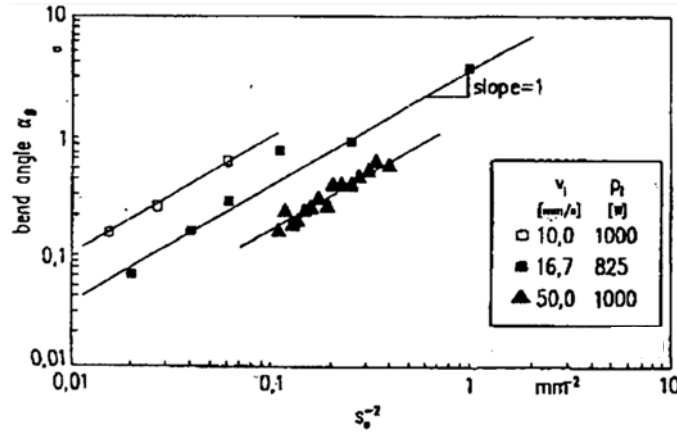
At the same time, both materials are insensitive to the laser source that is being used. While the laser wavelength can have a significant effect on the absorption coefficient (Steen and Mazumder, 2010), the absorption can generally be maintained at a high level by spray-painting the specimens with black graphite paint. Therefore, successful forming experiments can be conducted with many types of lasers, such as continuous-wave Nd:YAG lasers (Bucher et al., 2016), diode lasers (Guglielmotti et al., 2009), as well as pulsed CO<sub>2</sub> lasers (Roohi et al., 2015). Many different types of lasers have equally been used for sheet metal, such as for instance pulsed Nd:YAG lasers (Gollo et al., 2011) or continuous-wave CO<sub>2</sub> lasers (Li and Yao, 2000), again demonstrating the low impact of the laser type on the outcome of the process.

A new process parameter that comes into the picture when dealing with metal foams is the density. Metal foams can be manufactured over a large range of densities by changing the porosity and the cell wall thickness. With increasing foam density, the stiffness, flow stress, and thermal conductivity increase as was shown in equations (1)–(3), decreasing the temperature gradients and rendering the material more rigid to bending deformation. Moreover, with increasing cell wall thicknesses, the cell walls can bend less readily, decreasing the efficiency of the MTGM. Experiments have confirmed this finding as shown in Figure 11. Two open-cell metal foams with densities of 210 kg/m<sup>3</sup> (low) and 250 kg/m<sup>3</sup> (high) were tested under two different process conditions, and the low-density foam consistently yielded larger bending angles.

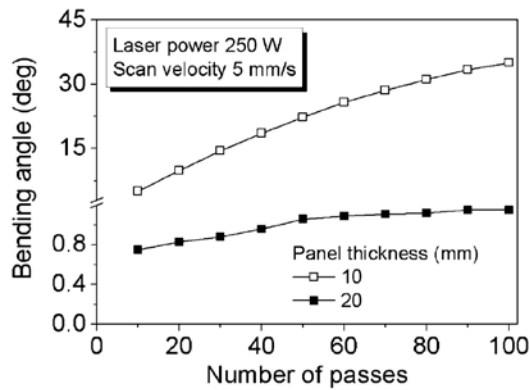
A further process condition that is important for metal foams, yet negligible for sheet metal, is the composition. Based on the current experimental results, it seems that the formability of metal foams is very sensitive to the composition, particularly the alloy elements. Thus far, successful bending results have only been reported with

aluminium-based foams that contain silicon and magnesium as major alloy elements. However, one study attempted laser forming of an aluminium-based alloy with 20 weight percent silicon carbide (SiC), yielding a negative result (Zhang et al., 2015). Bending angles reached barely 1°, and an excessive amount of melting and thermally induced damage was observed. Closer investigations revealed that the SiC significantly reduced the thermal expansion coefficient of the alloy, rendering laser forming nearly impossible. For solid metal sheets, the material composition seems to have less of an impact. Successful laser forming experiments were performed with a wide range of materials, such as steel, nickel, titanium, aluminium alloys, chromium, and silicon (Shen and Vollertsen, 2009).

**Figure 10** The bending angles decrease with increasing sheet thickness, both in solid and foamed metals



(a)



(b)

Notes: In solid metals, the bending angle is proportional to  $(s_0)^{-2}$  as shown in (a) (Vollertsen, 1994). In metal foams, doubling the thickness caused a drop in the bending angle by more than an order of magnitude, as shown in (b) (Guglielmotti et al., 2009).

**Figure 11** For an open-cell aluminium foam, higher bending angles were achieved at a low density ( $210 \text{ kg/m}^3$ ) than at a high density ( $250 \text{ kg/m}^3$ ) (Quadrini et al., 2010), suggesting an inverse relationship

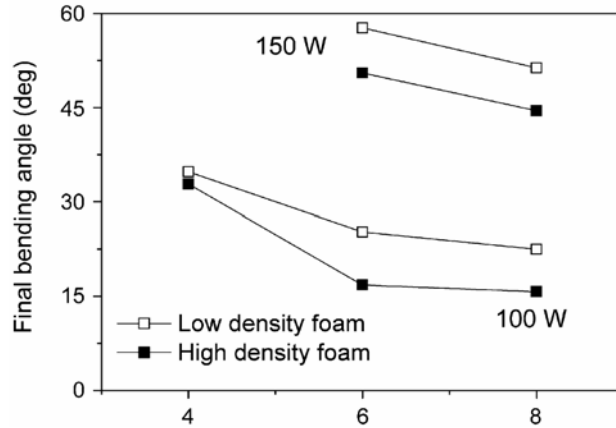


**Figure 12** Bending curves with and without cooling through a protective gas for (a) steel sheets (Cheng and Yao, 2001) and (b) closed-cell metal foams with protective skins (Guglielmotti et al., 2009)

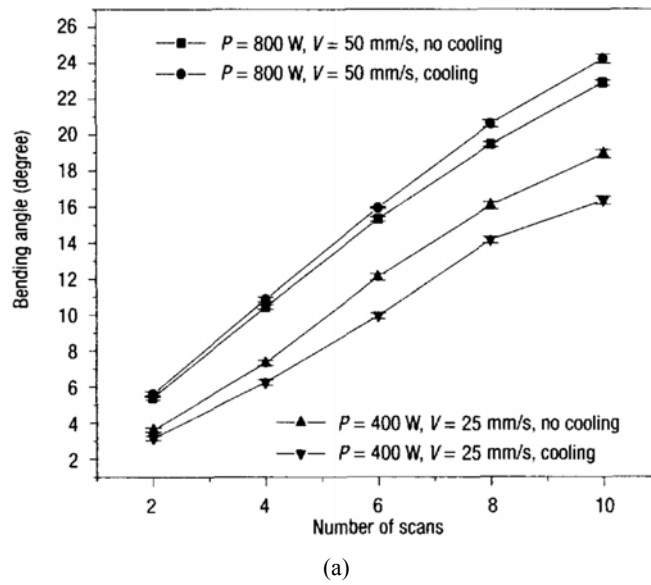
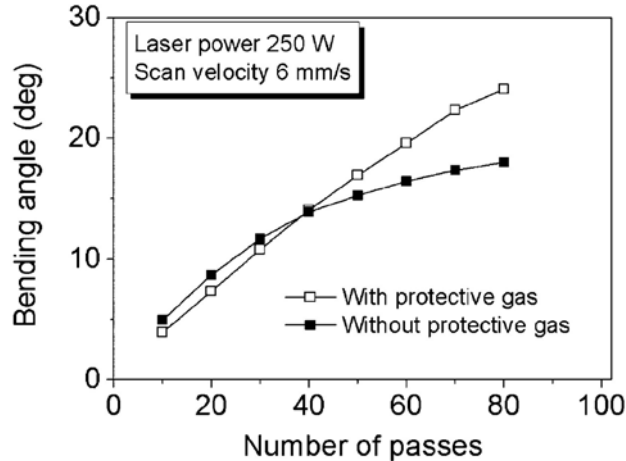


**Figure 12** Bending curves with and without cooling through a protective gas for (a) steel sheets (Cheng and Yao, 2001) and (b) closed-cell metal foams with protective skins (Guglielmotti et al., 2009) (continued)



(b)

Finally, metal foams are also more sensitive to the cooling condition than sheet metal. For sheet metal, it has been shown that in-process cooling has a negligible impact on the forming efficiency, microstructure, and the mechanical properties (Cheng and Yao, 2002). Cooling though increases the process productivity by reducing the cooling time between successive laser scans, yet has a relatively small impact on the bending angles [Figure 12(a)]. For metal foams, on the other hand, the cooling condition has a more significant impact on the formability. Guglielmotti et al. (2009) showed that in the absence of a cooling gas, the bending angle is initially higher because of the increased heat input [Figure 12(b)], but rapidly starts to drop with an increasing number of scans. The reason is that melting and over-heating (tarnishing) occur in the absence of the protective environment, which hardens the material and makes bending more difficult.

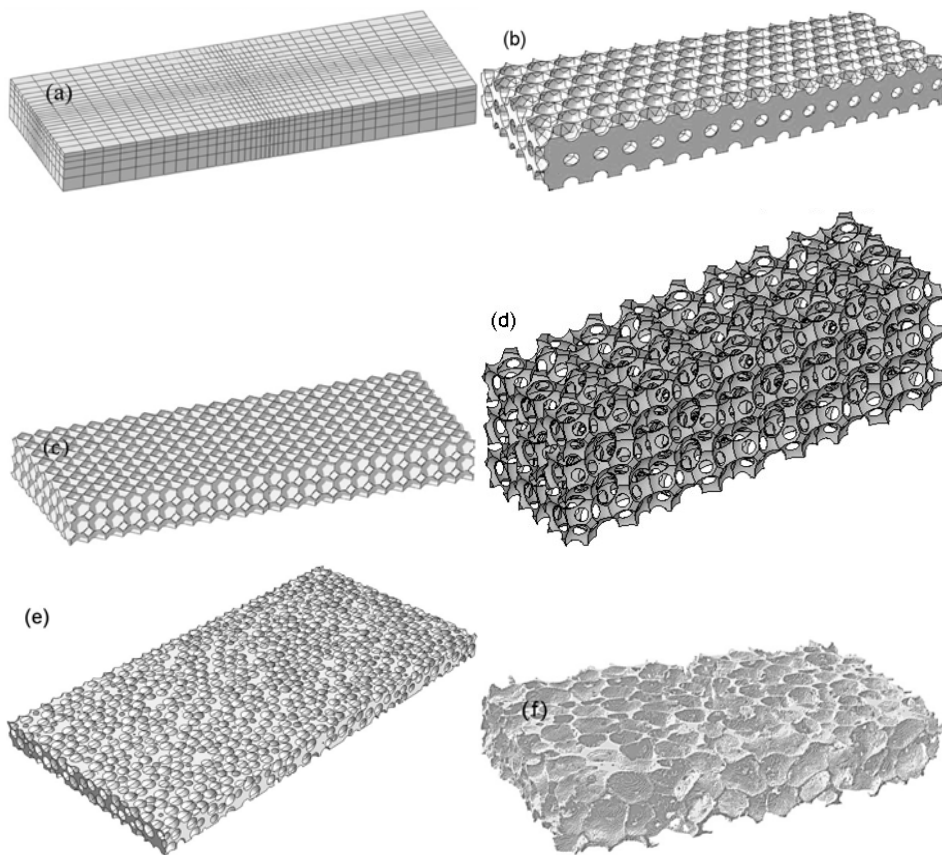
#### 4 Numerical simulation

Since the beginning of laser forming research, numerical simulations have been used as a powerful tool to predict the outcome of laser forming processes and to reduce experimental efforts. For laser forming of sheet metal, highly accurate numerical models have been developed, and many numerical aspects have been investigated that were summarised by Shen and Vollertsen (2009).

For laser forming of metal foam, comparatively little numerical work has been done. Most of the work has been focused on the key difference between the simulation of solid and foamed metal: the model geometry. Two main approaches have been used to model the foam geometry. In the first approach, the foam geometry is approximated by a solid rectangle, and metal foam properties are assigned to the model. Models following this approach are called 'equivalent' models, shown in Figure 13(a). In the second approach, the foam geometry is modelled explicitly, and properties are assigned of the solid that the

foam is comprised of models following this approach are called ‘explicit’ models, shown from Figures 13(b) to 13(f).

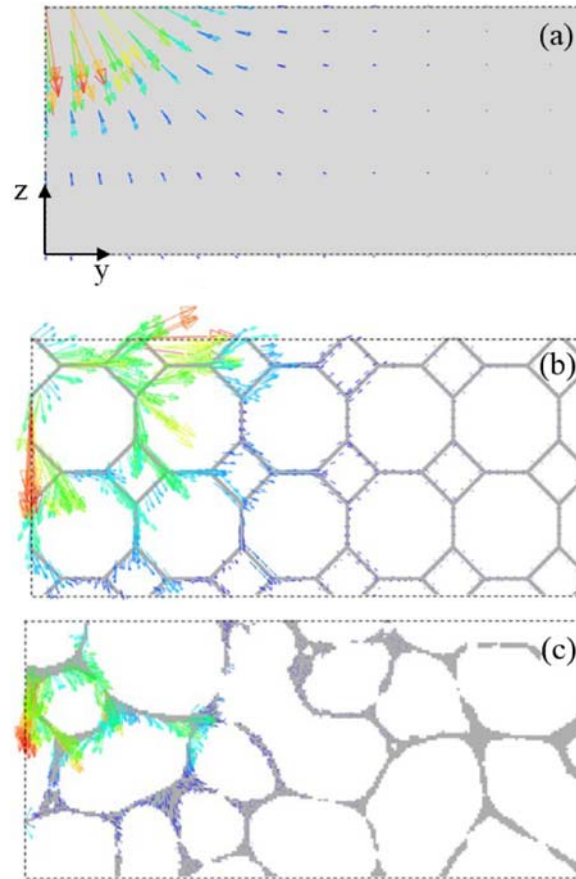
**Figure 13** The metal foam geometry can be approximated by a solid geometry (‘equivalent’ model) (Bucher et al., 2016), shown in (a) or modelled explicitly using different levels of geometrical approximation, shown from (b) to (f), (b) and (c) use spherical (Zhang et al., 2015) and Kelvin-cell based (Bucher et al., 2016) unit-cell approaches to model a closed-cell foam, respectively, (d) represents an open-cell model that was also established using a unit-cell approach (Santo et al., 2010), (e) shows a high-density foam model with randomly positioned cavities of different radii (Roohi et al., 2015) and (f) shows a closed-cell foam model that was obtained through a micro-CT scan (Bucher et al., 2016)



Equivalent models have the advantage of being extremely simple to implement. A comparatively small number of elements is required, hence computing times are low and multi-pass laser forming experiments are feasible up to large bending angles. At the same time, equivalent models require the specification of metal foam material data, which is challenging to obtain. Due to the ability of foams to yield in hydrostatic compression, the hydrostatic yield strength and the plastic Poisson’s ratio need to be specified as additional parameters, both of which require elaborate test procedures (Deshpande and Fleck, 2000). Furthermore, equivalent models induce errors due to their oversimplified geometry. The incoming laser source is entirely absorbed at the top

surface as shown in Figure 14(a), which differs from reality where the laser scan can penetrate into the cavities. The heat dissipation is unrealistic as well, since heat can distribute radially in an unrestricted manner.

**Figure 14** Heat flux vectors in cross sections of the (a) equivalent model, (b) Kelvin-cell model and (c) micro-CT-based model during laser irradiation (see online version for colours)



Notes: Legends are omitted since the plots are used for a qualitative comparison. Unlike in (a), the heat flux is channelled through thin cell walls in (b) and (c), and hence the heat transfer prediction is more realistic. (c) is most accurate since the cavity depth varies, and the heat flux is interrupted wherever cell walls are missing.

*Source:* Bucher et al. (2016)

Some of the shortcomings of the equivalent models can be overcome by using explicit models. Due to their cellular structure, the laser can penetrate into the cavities, and the heat flux is channelled through the cell walls [see Figure 14(b) and 14(c)]. Depending on the level of geometrical approximation, explicit models can be divided into three sub-categories. In the first sub-category, the cavity geometry is approximated by some unit-cell geometry, which is then repeated throughout the model. The easiest possible unit-cell shape is a sphere, and the corresponding model is shown in Figure 13(b). While

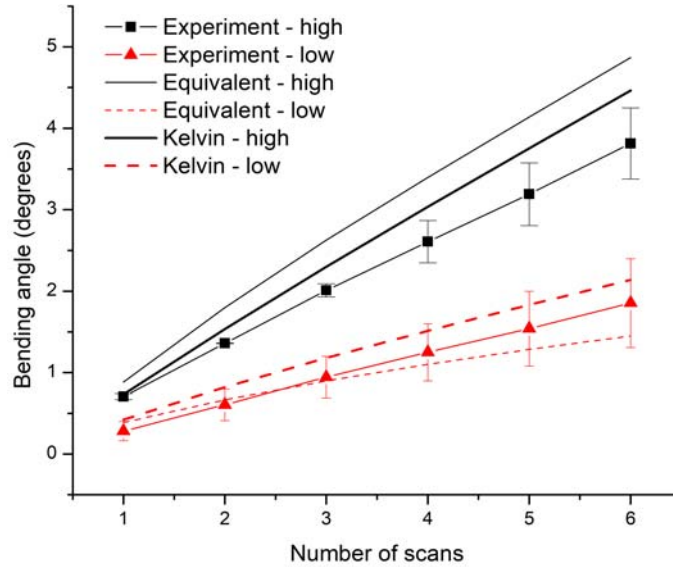
approximating the cavity shape rather well, a spherical-based model over-estimates the solid accumulations between cavities. The Kelvin-cell model, shown in Figure 13(c), solves this problem by using a stackable Kelvin-cell cavity geometry, which maintains a constant cell wall thickness throughout the model. Due to the constant wall thickness, the heat diffusion is slightly more accurate as can be seen from the heat flux vectors in Figure 14(b). Yet, the model slightly overestimates the laser absorption near the top surface (Bucher et al., 2016). Unit-cell based explicit models have also been developed for open-cell foams, as shown in Figure 13(d). Overall, unit-cell based models can be reasonably accurate, depending on the level of geometrical abstraction, but they generally fail to capture the randomness in the foam geometry.

Models of the second sub-category use similar geometrical abstractions as unit-cell based models, but introduce randomness in the cavity size and positions. Roohi et al. (2015) developed such a model for a high-density foam with a 30–70% porosity by randomly distributing spherical cavities with a range of different radii [Figure 13(e)]. Due to the randomisation of the cavity location and size, this approach has an improved geometrical accuracy compared to the unit-cell based models. Nevertheless, its accuracy is still limited because the cavity shape is approximated by spheres and thus does not capture the imperfections in the foam geometry. Moreover, this method can only be used for high-density foams, since the maximum achievable porosity with spherical cavity models is limited to roughly 75%.

The true randomness and imperfections of the foam geometry can only be captured by models of the third sub-category, where the foam geometry is reproduced ‘exactly’ using micro-computed tomography (micro-CT). The micro-CT scan yields a data cloud, which is converted to a solid model by replacing each data point by a cubical element, called ‘voxel’. If the micro-CT scan is performed with a high spatial resolution, a nearly perfect reproduction can be obtained of the foam structure. Due to the geometrical accuracy, the laser absorption is most realistic, and the model can capture openings in the cell walls where the heat flux is interrupted [Figure 14(c)]. Moreover, it can be predicted which cell walls are likely to undergo melting. Besides these advantages, the micro-CT model has two major drawbacks. First, each model only represents one single metal foam specimen, and a new model needs to be created for each specimen if a high model accuracy is desired. Second, the model is extremely CPU intensive. Even if only a small subset of the foam specimen is modelled, the number of elements can readily reach multiples of 100,000, rendering the mechanical part of the simulation prohibitively time intensive.

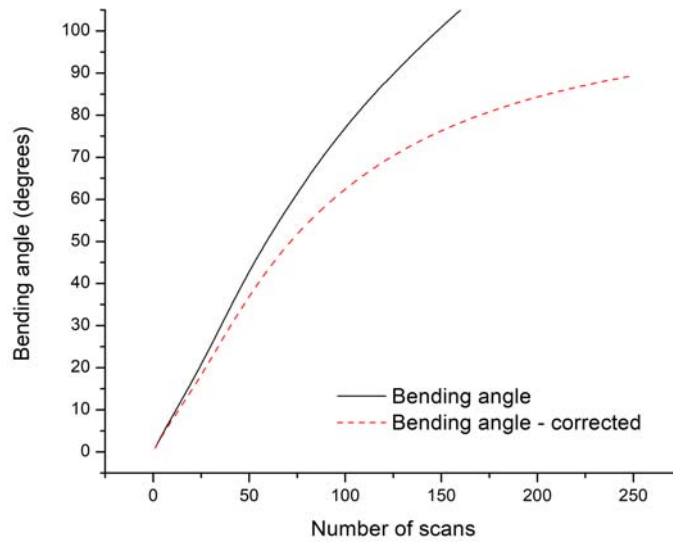
Overall, increasing the model geometry can to some degree improve the predictive accuracy. Figure 15 shows that the bending angles predicted by the Kelvin-cell model more closely matched experimental values than the angles predicted by the equivalent model. At the same time, this rather small increase in accuracy comes at a high computational cost. Whereas the equivalent model can be used to simulate laser forming processes up to 250 scans, the Kelvin-cell model can merely achieve 10 scans, and the micro-CT model is currently too CPU intensive to predict the angle of even a single laser scan. In most cases it is not necessary to go to the extreme of using elaborate micro-CT or unit-cell based models, since the equivalent model can make reasonably accurate predictions, especially if density-dependent material data from equations (1)–(3) is incorporated as shown in Figure 16.

**Figure 15** Comparison of experimental bending angles with bending angles predicted by an equivalent model and a Kelvin-cell model (see online version for colours)



Notes: Standard errors are shown for the experimental data. The predictions of the Kelvin-cell model are slightly closer to the experimental values, due to its higher geometrical accuracy.

**Figure 16** Large bending-angle results generated with the equivalent model (see online version for colours)

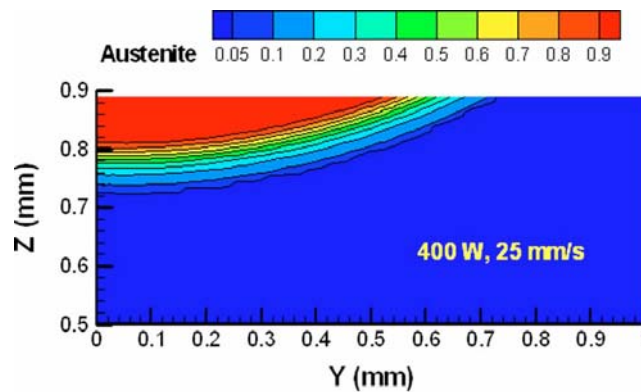


Notes: If density-dependent material data is not incorporated into the model, the bending angle increases continuously, which does not match experimental observations. If density-dependent data is incorporated (corrected), on the other hand, the model can capture the plateau behaviour observed in the experimental data in Figure 7(b).

Regardless of the model geometry, numerical foam models of all kinds predict similar material responses as numerical models of sheet metal. Both models for instance predict an initial counter-bending due to the slight expansion of the heated material before the onset of plastic deformation (Vollertsen, 1993; Quadrini et al., 2013). Both models also predict similar plastic strain distributions, as was shown in Figure 6.

Some aspects that have been included in sheet metal simulations have not yet been included in metal foam simulations, either because they become negligible, or because they are difficult to implement. A first aspect involves incorporating strain-dependent material data. In sheet metal laser forming, the strain rates can become sizeable (up to  $2 \text{ s}^{-1}$ ) during the heating and cooling cycles, which can significantly increase the flow stress of the treated material and reduce the bending angle (Li and Yao, 2000). In metal foam laser forming, however, the strain rates are typically an order of magnitude smaller due to the reduced scan speed ( $\sim 0.2 \text{ s}^{-1}$ ), and thus incorporating strain-rate dependent material data has a negligible impact.

**Figure 17** Volume fraction of transformed austenite in a low-carbon steel sheet at the end of laser heating (see online version for colours)



Note: Knowing the phase distribution, phase-specific material data can be assigned.

Source: Fan et al. (2007)

The second aspect relates to the incorporation of micro-structural changes that occur during laser scans. This has been done for simulations of steel sheets and Ti-6Al-4V, where the formation of different phases was predicted based on the maximum temperatures and cooling rates that occur during the laser scan (Cheng and Yao, 2002; Fan et al., 2007). Figure 17, for instance, shows the predicted volume fraction of transformed austenite in a low-carbon steel sheet at the end of heating. Once the different phases are known that coexist during and after the laser scan, phase-specific material data can be assigned to the model, thereby increasing the model accuracy. In metal foams, micro-structural changes can occur as well; (Santo et al., 2012), for instance, reported a refinement of the eutectic Al-Si structure within the heat-affected zone of an AlSi7Mg foam. Despite having observed micro-structural changes, however, they have not yet been incorporated in numerical models, for several reasons. First, all metal foams that have been investigated so far were aluminium-based. The micro-structure of Al-alloys is often complicated and includes many types of precipitates and secondary phases, for which material data is not readily available. Second, micro-structural changes do not

occur uniformly as in solid metal sheets. Due to the irregular foam structure, some thin cell walls might undergo a phase change more quickly than the material in an accumulated area between foam cells. Therefore, it is far more challenging to model micro-structural changes for metal foams.

## 5 Future work

From the previous three sections it can be seen that much progress has been made towards a better understanding of laser forming of metal foam. Yet, many aspects require further investigation, both experimentally and numerically.

Experimentally, more data needs to be acquired for aluminium-based metal foams with alloy elements different than silicon and magnesium. Furthermore, laser forming experiments yet have to be conducted with metal foams that consist of different base metals than aluminium, such as magnesium and titanium. Thereby it needs to be investigated whether the foam composition has an impact on the bending mechanism. No work has also been done in 3D-forming of metal foam panels and 3D process synthesis, an area that is well-understood in sheet metal laser forming (Cheng and Yao, 2004; Edwardson et al., 2005a).

Numerically, a method needs to be developed to reduce the number of elements of micro-CT based models without sacrificing their geometrical accuracy, possibly by using marching-cube algorithms that convert the micro-CT data cloud into a smooth mesh (Lorensen and Cline, 1987). Overall, elaborate explicit models are expected to become increasingly feasible and valuable as the computational power is improving. Incorporating micro-structural effects into the numerical foam models is expected to become more important, particularly if the investigations are expanded to steel-based foams. Also, fully coupled thermo-mechanical models need to be developed that are capable of simulating multiple scans up to large bending angles. Thus far, such models have only been used for single scans (Roohi et al., 2015). At large bending angles, changes in the laser absorption and the thermal conductivity become significant [see equation (3)], which can only be taken into account by fully coupled models.

Further work is currently underway in laser forming of sandwich composites. Sandwich composites consist of metal foam sheets that are sandwiched between two sheet metal plates. The metal sheets not only protect the foam core, but also generate a structurally strong composite with a superior stiffness and excellent shock absorption properties. The study of sandwich composite laser forming is rather involved and requires an expertise in both foamed and solid metal laser forming. The solid-foam interaction renders the bending mechanism analysis more complicated, and several numerical challenges are introduced due to the presence of the solid-foam interface.

## 6 Conclusions

This paper reviewed the research efforts made in the field of laser forming of metal foams and compared the current knowledge with the well-established knowledge in sheet metal laser forming. It was shown that the bending mechanisms from sheet metal laser forming either do not apply to metal foams, or require modification. Moreover, the process window applicable to metal foam was shown to be a subset of the process

window applicable to sheet metal, and the reasons were discussed. It was shown that the major difference between the numerical simulation of foamed and solid metals relates to the model geometry, and different approaches were presented to model the metal foam geometry. Finally, subjects requiring further study were reviewed.

Overall, it was shown that a good fundamental understanding has been developed of laser forming of metal foam. Compared to sheet metal laser forming, however, the knowledge still contains gaps. More experimental and numerical results need to be obtained to enable a safe and reliable application of laser formed metal foam products in industry.

### Acknowledgements

The financial support from the National Science Foundation under a GOALI grant #CMMI-1725980 is gratefully acknowledged.

### References

- Ashby, M.F., Evans, A.G., Fleck, N.A., Gibson, L.J., Hutchinson, J.W. and Wadley, H.N.G. (2000) *Metal Foams: a Design Guide*, Butterworth-Heinemann, Washington DC.
- Banhart, J. (2001) 'Manufacture, characterisation, and application of cellular metals and metal foams', *Progress in Materials Science*, Vol. 46, No. 6, pp.559–632.
- Bucher, T., Bolger, C., Zhang, M., Chen, C. and Yao, Y.L. (2016) 'Effect of geometrical modeling on prediction of laser-induced heat transfer in metal foam', *Journal of Manufacturing Science and Engineering*, Vol. 138, No. 12, p.121008.
- Bucher, T., Young, A., Zhang, M., Chen, C. and Yao, Y.L. (2017) 'Bending mechanism analysis for laser forming of metal foam', *Proceedings of the Manufacturing Science and Engineering Conference*, Blacksburg, Virginia, USA.
- Cheng, J. and Yao, Y.L. (2001) 'Cooling effects in multi-scan laser forming', *Journal of Manufacturing Processes*, Vol. 3, No. 1, pp.60–72.
- Cheng, J. and Yao, Y.L. (2002) 'Microstructure integrated modeling of multiscan laser forming', *Journal of Manufacturing Science and Engineering*, Vol. 124, No. 2, p.379.
- Cheng, J. and Yao, Y.L. (2004) 'Process synthesis of laser forming by genetic algorithms', *International Journal of Machine Tools and Manufacture*, Vol. 44, No. 15, pp.1619–1628.
- Claar, T.D., Yu, C.J., Hall, I., Banhart, J., Baumeister, J. and Seeliger, W. (2000) 'Ultra-lightweight aluminum foam materials for automotive applications', *SAE Technical Paper Series*, Detroit, Michigan, USA, pp.1–9.
- D'Urso, G. and Maccarini, G. (2011) 'The formability of aluminum foam sandwich panels', *International Journal of Material Forming*, Vol. 5, No. 3, pp.243–257.
- Deshpande, V. and Fleck, N. (2000) 'Isotropic constitutive models for metallic foams', *Journal of the Mechanics and Physics of Solids*, Vol. 486, No. 7, pp.1253–1283.
- Edwardson, S.P., Abed, E., French, P., Dearden, G. and Watkins, K.G. (2005a) 'Developments towards controlled three-dimensional laser forming of continuous surfaces', *Journal of Laser Applications*, Vol. 17, No. 4, pp.247–255.
- Edwardson, S.P., French, P., Dearden, G., Watkins, K.G. and Cantwell, W.J. (2005b) 'Laser forming of fibre metal laminates', *Lasers in Engineering*, Vol. 15, No. 3, pp.233–255.
- Edwardson, S.P., Abed, E., Bartkowiak, K., Dearden, G. and Watkins, K.G. (2006) 'Geometrical influences on multi-pass laser forming', *Journal of Physics D: Applied Physics*, Vol. 39, No. 2, pp.382–389.

- Fan, Y., Yang, Z., Cheng, P., Eglund, K. and Yao, Y.L. (2007) 'Investigation of effect of phase transformations on mechanical behavior of AISI 1010 steel in laser forming', *Journal of Manufacturing Science and Engineering*, Vol. 129, No. 1, p.110.
- Gibson, L.J. and Ashby, M.F. (1988) *Cellular Solids: Structure & Properties*, Pergamon, Oxford, UK.
- Gollo, M.H., Mahdavian, S.M. and Naeini, H.M. (2011) 'Statistical analysis of parameter effects on bending angle in laser forming process by pulsed Nd:YAG laser', *Optics & Laser Technology*, Vol. 43, No. 3, pp.475–482.
- Guglielmotti, A., Quadrini, F., Squeo, E.A. and Tagliaferri, V. (2009) 'Laser bending of aluminum foam sandwich panels', *Advanced Engineering Materials*, Vol. 11, No. 11, pp.902–906.
- Haijun, Y. (2007) *Research on Acoustic, Mechanical and Other Properties of Closed-Cell Aluminum Foam*, Unpublished PhD thesis, Northeastern University, Shenyang, Liaoning, China.
- Kennedy, A. (2012) 'Porous metals and metal foams made from powders', in Kondoh, K. (Ed.): *Powder Metallurgy*, InTech, Rijeka, Croatia, pp.31–46.
- Li, W. and Yao, Y.L. (2000) 'Numerical and experimental study of strain rate effects in laser forming', *Journal of Manufacturing Science and Engineering*, Vol. 122, No. 3, p.445.
- Li, W. and Yao, Y.L. (2001a) 'Laser bending of tubes: mechanism, analysis, and prediction', *Journal of Manufacturing Science and Engineering*, Vol. 123, No. 4, pp.674–681.
- Li, W. and Yao, Y.L. (2001b) 'Laser forming with constant line energy', *The International Journal of Advanced Manufacturing Technology*, Vol. 17, No. 3, pp.196–203.
- Li, W. and Yao, Y.L. (2001c) 'Numerical and experimental investigation of convex laser forming process', *Journal of Manufacturing Processes*, Vol. 3, No. 2, pp.73–81.
- Lorensen, W.E. and Cline, H.E. (1987) 'Marching cubes: a high resolution 3D surface construction algorithm', *Computer Graphics*, Vol. 21, No. 4, pp.163–169.
- Masubuchi, K. and Jones, J.E. (2000) 'Laser forming for flexible fabrication', *Journal of Ship Production*, Vol. 16, No. 2, pp.97–109.
- Mata, H., Santos, A., Parente, M., Valente, R., Fernandes, A. and Jorge, N. (2013) 'Study on the forming of sandwich shells with closed-cell foam cores', *International Journal of Material Forming*, Vol. 7, No. 4, pp.413–424.
- Mondal, D.P., Ramakrishnan, N., Suresh, K.S. and Das, S. (2007) 'On the moduli of closed cell aluminum foam', *Scripta Materialia*, Vol. 57, No. 10, pp.929–932.
- Pretorius, T. (2009) 'Laser forming', in Dowden, J. and Schultz, W. (Eds.): *The Theory of Laser Materials Processing: Heat and Mass Transfer in Modern Technology*, pp.281–314, Springer, Dordrecht.
- Quadrini, F., Bellisario, D., Ferrari, D., Santo, L. and Santarsiero, A. (2013) 'Numerical simulation of laser bending of aluminum foams', *Key Engineering Materials*, Vols. 554–557, pp.1864–1871.
- Quadrini, F., Guglielmotti, A., Squeo, E.A. and Tagliaferri, V. (2010) 'Laser forming of open-cell aluminium foams', *Journal of Materials Processing Technology*, Vol. 210, No. 11, pp.1517–1522.
- Roohi, A.H., Naeini, H.M., Gollo, M.H., Soltanpour, M. and Abbaszadeh, M. (2015) 'On the random based closed-cell metal foam modeling and its behavior in laser forming process', *Optics & Laser Technology*, Vol. 72, pp.53–64.
- Santo, L., Bellisario, D., Rovatti, L. and Quadrini, F. (2012) 'Microstructural modification of laser-bent open-cell aluminum foams', *Key Engineering Materials*, Vols. 504–506, pp.1213–1218.
- Santo, L., Guglielmotti, A. and Quadrini, F. (2010) 'Formability of open-cell aluminium foams by laser', *Proceedings of the Manufacturing Science and Engineering Conference*, Erie, Pennsylvania, USA, pp.1–8.
- Scully, K. (1987) 'Laser line heating', *Journal of Ship Production*, Vol. 3, No. 4, pp.237–246.

- Shen, H. and Vollertsen, F. (2009) 'Modelling of laser forming – an review', *Computational Materials Science*, Vol. 46, No. 4, pp.834–840.
- Shi, Y., Yao, Z., Shen, H. and Hu, J. (2006) 'Research on the mechanisms of laser forming for the metal plate', *International Journal of Machine Tools and Manufacture*, Vol. 46, Nos. 12–13, pp.1689–1697.
- Steen, W.M. and Mazumder, J. (2010) *Laser Material Processing*, Springer, London, UK.
- Vollertsen, F. (1993) 'The mechanisms of laser forming', *Proceedings of the International Laser Assisted Net Shape Engineering Conference*, Meisenbach Bamberg, Germany, pp.301–304.
- Vollertsen, F. (1994) 'An analytical model for laser bending', *Lasers in Engineering*, Vol. 2, pp.261–276.
- Zhang, M., Chen, C.J., Brandal, G., Bian, D. and Yao, Y.L. (2015) 'Experimental and numerical investigation of laser forming of closed-cell aluminum foam', *Journal of Manufacturing Science and Engineering*, Vol. 138, No. 2, p.021006.
- Zu, G.Y., Lu, R.H., Li, X.B., Zhong, Z.Y., Ma, X.J., Han, M.B. and Yao, G.C. (2013) 'Three-point bending behavior of aluminum foam sandwich with steel panel', *Transactions of Nonferrous Metals Society China*, Vol. 23, No. 9, pp.2491–2495.

### Nomenclature

$\alpha_B$	Bending angle	$A$	Absorption coeff.
$\alpha_{th}$	Thermal exp. coeff.	$B_1$	Scaling factor
$c_p$	Specific heat	$D$	Spot size
$k$	Thermal conductivity	$E$	Young's modulus
$l$	Beam length	$Fo$	Fourier number
$\rho$	Density	$I$	Moment of area
$S_0$	Sheet thickness	$P$	Power
$v$	Scan speed		
$\nu$	Poisson's ratio		
$y$	Y – coordinate		
$z$	Z – coordinate		
$\phi$	Perc. solid at cell intersec.		